Practical approaches for evaluating bending and torsion of fiber-reinforced polymer components using instrumented testing

Isaac L. Howard
Mississippi State University
ilhoward@cee.msstate.edu

ABSTRACT

This paper discusses instrumented testing of Fiber Reinforced Polymer (FRP) materials for constructing lightweight bridge decks. Torsion and bending tests are performed on multi-cellular components to evaluate the torsional constant (polar moment of inertia of the section), influence of simultaneous loadings on elastic properties, and the effect of shear forces on the total deflection. A practical approach is taken in the absence of extensive theoretical computations. The methods employed performed well and are a combination of instrumented testing and fundamental mechanics principles.

INDEX TERMS

Bridge decks, Fiber reinforced polymers, Instrumented testing, Shear deflection

I. INTRODUCTION

The bridge infrastructure of the United States (likely other countries as well) is in need of technology and materials to allow economical solutions to a deteriorating portion of the country's transportation system. Recent highly-publicized bridge failures exacerbate these needs. FHWA [1] reports 26.7% of the nation's bridges are structurally deficient and/or functionally obsolete. This value has declined slightly from previous years, but still requires further reduction. A common cause of bridge deficiency is corrosion caused by a combination of the natural environment and de-icing chemicals.

Fiber Reinforced Polymer (FRP) is a material showing promise to improve bridge infrastructure. Pultruded FRP materials are capable of producing quality products with complicated fiber architectures provided key factors, such as pull forces and speeds, are controlled [2]. West Virginia is one of the leaders in implementing thin-walled-lightweight FRP bridge decks (e.g., [3]).

Advantages of FRP material in bridge deck applications include:

1. High tensile strength to density ratio;
2. High stiffness to density ratio;
3. Non-corrosive constituents; and
4. Ability to tailor properties to the desired
5. application.

Disadvantages of FRP material in bridge deck applications include:

1. Greater level of engineering understanding needed to effectively use anisotropic materials;
2. More shear lag compared to conventional metals; and
3. Higher initial cost.

Long span bridges are of particular interest to FRP materials, while one must remain mindful of their modest elastic moduli (especially shear moduli), which can result in designs driven by deflection and buckling [4].

Materials such as FRP can be tested at three levels:

1. *Coupon*-small piece cut away from manufactured product;
2. *Component*-complete manufactured product; and
3. *System*-multiple FRP components attached together and used in conjunction with other

structural components (e.g., steel or other FRP's).

This paper focuses on *component*-level evaluation, while companion papers detail *system*-level testing of the same components. Two thin-walled multi-cellular FRP deck components containing E-glass fibers were evaluated (Figure 1). Both were similar in geometry and fiber constituents, but one was made using a polyester resin matrix while the other used a vinylester resin matrix. Their fiber volume fraction was approximately 54%, with the mass being approximately 73 kg/m^3 of deck area and the thickness of the walls within a component being between 6.4 to 12.7 mm.

The objective of this paper is to present *component*-level instrumented testing of the two aforementioned FRP deck materials and incorporate the results into straightforward theoretical computations. The work presented shows instrumented testing coupled with sound fundamental principles can provide reasonable solutions to extremely complicated problems involving shear lag, stress concentration, three-dimensional stress states, and thin-walled anisotropic specimens.

II. APPROXIMATE CLASSICAL LAMINATION THEORY

Approximate Classical Lamination Theory (ACLT) is a simplified version of Classical Lamination Theory (CLT). Both may be used to determine the in-plane bending and shear stiffness of a composite component. Extensive work regarding ACLT is contained in [5] and is the basis for much of the information presented in this section.

The general approach uses superposition to compute the moduli and subsequent stiffness properties of each lamina in the composite and sums them to determine the overall value. The elastic moduli in a given direction are computed from (1) and (2).

$$E_x \approx E_{11}\cos^4(\theta)$$

$$E_y \approx E_{11}\cos^4(90-\theta) \qquad (2)$$

$E_{x,y}$ are lamina moduli in the directions seen in Figure 1(b), and θ is the fiber orientation with respect to the *X*-axis of Figure 1(b). Equations (3) through (7) calculate all bending stiffness properties of the composite and result in the global bending stiffness (*EI*) of the component. Equation (5) was taken from [6], and equation (6) was taken from [7].

$$A_f = A_w = b\sum_{k=1}^{N}(E_t)_k t_k \qquad (3)$$

$$B_f = B_w \approx b\sum_{k=1}^{N}(E_t)_k t_k Z_k \qquad (4)$$

$$D_f \approx b\sum_{k=1}^{N}(E_t)_k\left[t_k Z_k^2 + \frac{t_k^3}{12}\right] \qquad (5)$$

$$D_w \approx b\sum_{k=1}^{N}(E_t)_k\left[\left(\frac{t_k^3}{12}+t_k Z_k^2\right)\cos^2(\varphi)+\left(\frac{b^2 t_k}{12}\right)\sin^2(\varphi)\right] \qquad (6)$$

$$EI \approx \sum_{f=1}^{n}\left[D_f + A_f e_f^2\right]+\sum_{w=1}^{m}\left[D_w + A_w e_w^2\right] \qquad (7)$$

$A_{f,w}$ are the in-plane stiffness terms; b is the lamina width; t is the lamina thickness; $B_{f,w}$ are the extensional-bending coupling stiffness; Z_k is the distance of mid-surface of kth lamina from the centroid of the section; $D_{f,w}$ are the flange and web-bending stiffness: φ is the angle of orientation of any member with respect to the horizontal; *EI* is the global bending stiffness; and $e_{f,w}$ are the eccentricity from the mid-surface of the component.

The general form of the global shear stiffness in the *Y-Z* plane displayed in Figure 1(a) can be calculated using (8).

$$G_{yz}A = d\sum_{k=1}^{N}(G_y)_k t_k \qquad (8)$$

$G_{yz}A$ is the global shear stiffness in the *Y-Z* plane of Figure 1(a); d is the laminate depth; and G_y is the shear modulus which varies depending on the lamina type and fiber orientation (see [8] for more information). While the equations shown for bending and shear properties appear cumbersome, they are very user friendly and can easily be programmed into a spreadsheet for routine practical use.

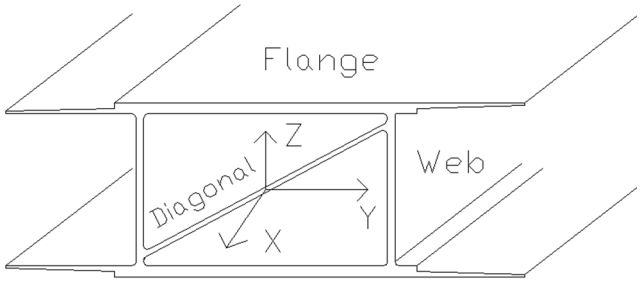

(a) General shape under investigation

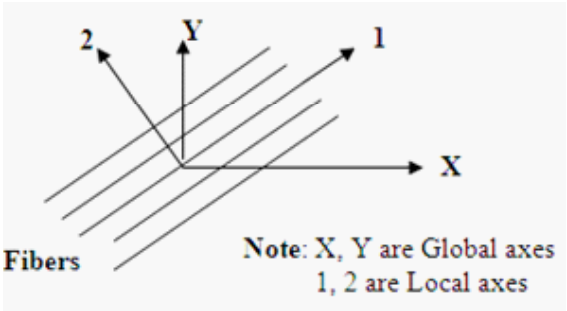

(b) Coordinate system for lamina fibers

Figure 1. General shape of FRP components and fiber coordinate system

Table I. Summarizes properties of both components calculated using the ACLT approach

Table I. ACLT calculation results for the FRP components

Component	$EI_{(x)}$ N*m^2	$EI_{(y)}$ N*m^2	$E_{(x)}$ Pa	$E_{(y)}$ Pa	$GA_{(yz)}$ N	$G_{(yz)}$ Pa
Polyester	3.91E+06	0.55E+06	30.96E+09	7.79E+09	1.96E+07	6.21E+09
Vinylester	3.01E+06	0.46E+06	24.13E+09	6.55E+09	2.13E+07	5.93E+09

III TORSION

Component-level torsional effects on thin-walled, closed sections were studied by [9]. Theoretical formulations were developed, but they were mostly for isotropic (rather than anisotropic or orthotropic) materials. The author stated that *component*-level shear stiffness must be obtained with great care. Furthermore, theoretical solutions for shapes, such as standard wide- flange sections, have existed for some time (e.g., [10]). Therein, solutions for the Saint-Venant torsional rigidity GJ are available, in addition to approximations of the torsion constant J (polar moment of inertia of the section). For a shape such as that shown in Figure 1, the problem is exceedingly more complex. A practical method to approximate J is presented in the remainder of this section.

Torsion testing of the polyester FRP bridge deck component was performed as shown in Figure 2. A load P was applied between a fixed distribution beam and a rigid beam connected to the free rotating ends of the load frame via turnbuckles. The rotation point of the free rotating ends aligned with the center of the FRP component being tested, which was a distance X from the turnbuckle.

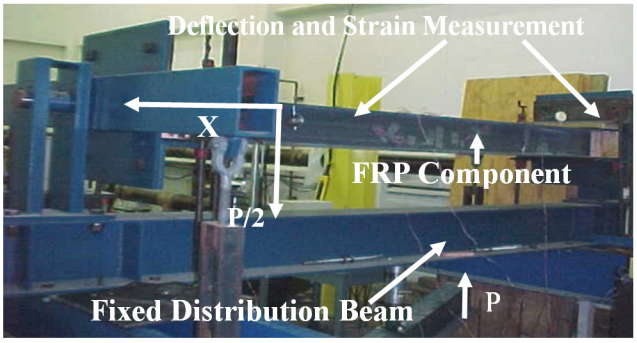

Figure 2. Torsion testing of FRP deck component

The specimen was clamped 0.2 m along its length on each end, and the clear span of the specimen was approximately 2.64 m. Foil strain gages and dial gages were used to instrument the specimen. Strain and deflection were measured 0.4 m from the fixities of both ends to ensure repeatability, making the distance between measurements 1.85 m. Force was applied at a rate of 2.2 kN/min. The maximum strain recorded on the diagonal (a small hole was drilled to allow instrumentation onto the diagonal that can be seen in Figure 1) at the center of the span was 19 με indicating practically zero distortion at the center of the specimen. The strain increased up to 67 με on the specimen webs (Figure 1) at the location of deflection measurement, indicating relatively small amounts of actual distortion of the closed portion of the specimen. The amount of distortion of the material outside the closed portion would likely have been higher; thus, reducing its ability to resist torsional deformation.

Equations (9) through (11) were used to reduce the torsion test data and determine the shear stiffness in the Y-Z plane of Figure 1.

$$T = \frac{PX}{2}$$

(10) $$\varphi_i = \sin^{-1}\left[\frac{\psi_i}{b'}\right]$$

(11) $$K_{yz} = \left(\frac{\Delta T}{\Delta \varphi_{avg}}\right)\left(L'\right)$$

T is the torque applied at each end of the specimen; P is the applied load (Figure 2); X is the distance from the turnbuckle applying torque to the center of the specimen (Figure 2); φ_i is the angle of twist at point i expressed in radians; ψ_i is deflection at point i; b is lateral distance from specimen centerline to deflection measurement; ΔT is the change in torque during testing; $\Delta\varphi_{avg}$ is the average angle of twist during testing; and K_{yz} is the torsional stiffness defined in Figure 3(a), which plots the results of testing and determines K_{yz} to be 1.96E+06 N*m^2.

The diagonal member (Figure 1) would pose particular complexity in terms of deriving a theoretical solution for J. Using the ACLT calculated value of G_{yz} (6.21E+09) seen in Table 1, J is estimated to be 3.16E-04 m^4. This value is less than the algebraic sum of the moment of inertia of the specimen about both its axes (5.37E-04 m^4), which would be expected due to the influences of several phenomena.

IV COMBINED TORSION AND BENDING

Bending tests were performed at increased torque levels to determine if the FRP component could handle multiple-load types in the elastic range. Theoretical computations of such behavior would be challenging due to many facets, including the specimen geometry (idealized in Figure 1). The ability to isolate behaviors (e.g., torsion and bending) for the purposes of design is important for a bridge deck since its plate-like shape is routinely subjected to wheel loads potentially inducing bending and torsion in multiple directions simultaneously.

The test set up for combined torsion and bending is similar to Figure 2 except an additional load actuator is placed between the fixed-distribution beam and the FRP component to apply bending loads at a rate of 4.4 kN/min at the center of the span. To perform the test, the desired level of torsion was achieved by increasing the force from the actuator seen in Figure 2 at a rate of 2.2 kN/min, and once achieved, the torsion was held constant while the bending loads were applied.

Four different levels of torque were tested between 3,050 and 5,300 N*m, and the applied- bending-load versus strain for all data has been plotted in Figure 3(b) and Figure 3(c). As seen, the level of torque has no meaningful bearing on the load-versus-strain curve in either Figure 3(b) or Figure 3(c) as evidenced by the trend lines. If there was an effect, noticeable scatter would be present. This is a positive finding that provides evidence that these types of loadings can be analyzed separately in FRP deck design.

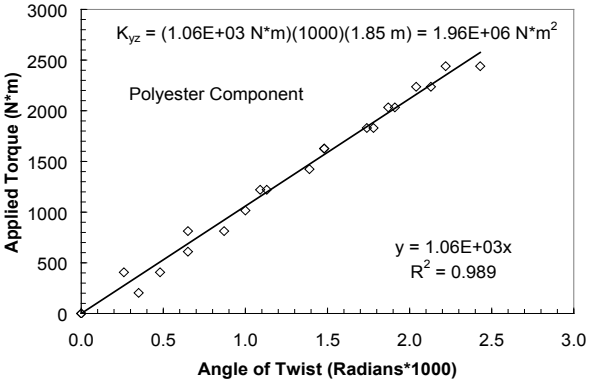

(a) Torque vs. Angle of Twist

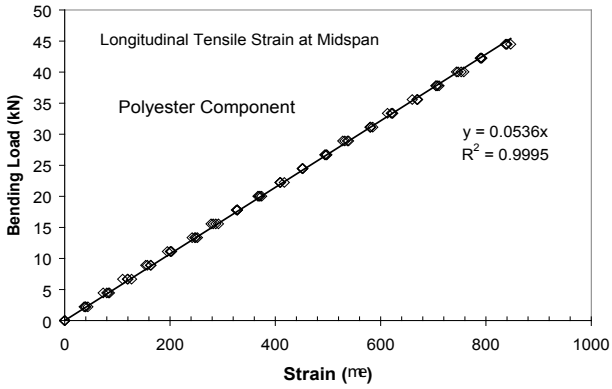

(b) Load vs. Long. Strain: Varying Torque

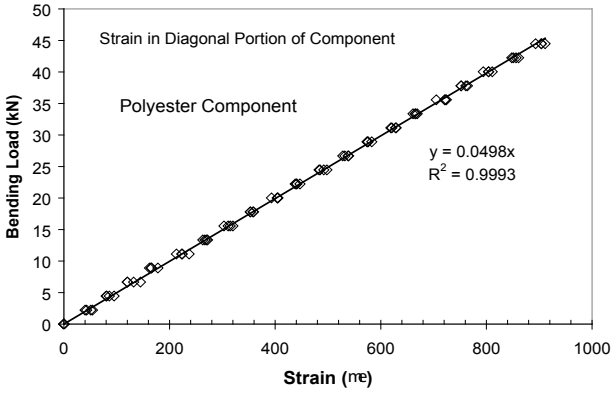

(c) Load vs. Diagonal Strain: Varying Torque

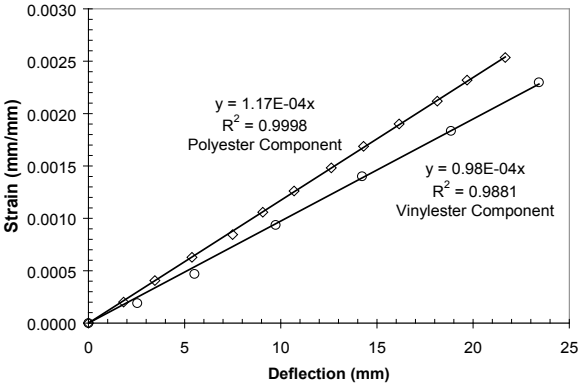

(f) Strain vs. Deflection

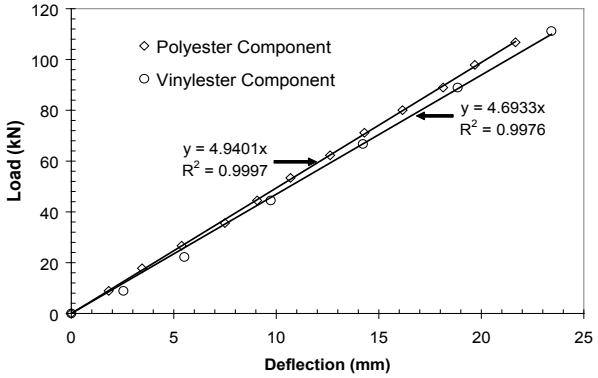

(d) Load vs. Deflection

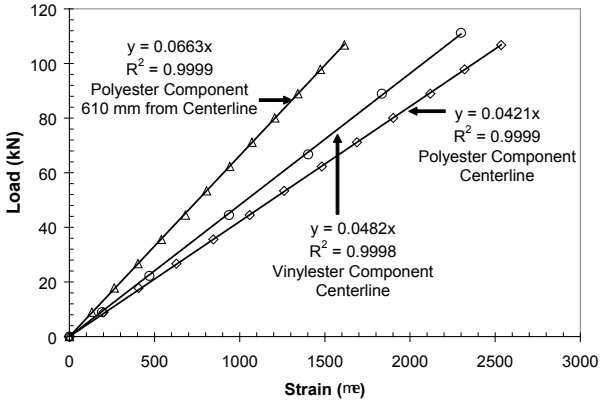

(e) Load vs. Strain

Figure 3 - Results of instrumented testing

V. BENDING

Previous research has dealt with deformation due to shear and its effect on pultruded FRP components. The problematic nature of FRP shear deflection and shear lag are highlighted by [11]. Highly complex theoretical predictions of shear coefficients of standard shapes are presented in [12] and [13]. Usal et al., [13] perform a rigorous derivation using deflection theories to decouple deflections due to shear and flexure (bending). Bank [14] recommends accounting for shear deflection in thin-walled composite components when the (L/r) ratio is less than 60, where L is the span length, and r is the radius of gyration. Bank [14] also recommends beam (component) level moduli to be used for deflection computations. Nagaraj and GangaRao [6] showed shear deflection to be significant in box and wide-flange shapes. An (L/r) ratio of 28 resulted in 36% of the total deflection due to shear in three-point bending tests.

The (L/r) ratio for the testing program presented in this paper is approximately 40, and the influence of shear deflection is readily observed. A practical method to determine the amount of shear deflection is presented using instrumented laboratory testing. Bending tests were conducted under simply supported conditions and a 3.048 m clear span (Figure 4). Wooden blocks were placed at the supports to prevent crushing, and 610 mm long wooden blocks were placed between the unsupported portions of the outside flanges to mimic the adjacent components that would be present in an actual bridge deck. Note the blocks were not wedged tightly into the outer portions of the out-

side flange, rather were fairly loose initially to avoid adding bending stiffness unrepresentative of in-service decks. They were included only to prevent excessive warping that would not occur with adjacent deck components in place.

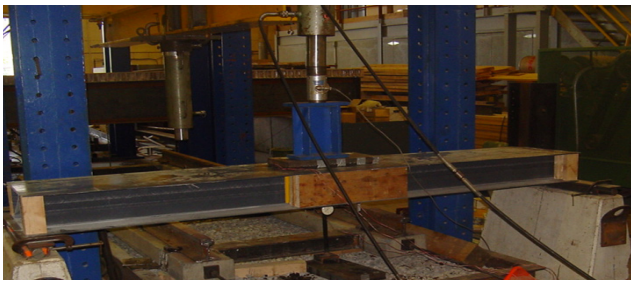

Figure 4. Test set up for bending experiments

Load-versus-deflection plots for both types of components are shown in Figure 3(d). As seen, they are linear, but the slopes differ somewhat. Figure 3(e) plots load versus strain of both types of components at the centerline of the specimen, and also plots the strain 610 mm from the centerline of the polyester component as a reference (strain considerably less but still consistent and linear). As in Figure 3(d), the slopes of the two component types differ somewhat. It is interesting to note that in terms of deflection, the vinylester component has a lower slope (relative to the polyester component) when plotted in terms of deflection than when plotted in terms of strain. This behavior is even more clearly demonstrated by considering Figure 3(f) in conjunction with the discussion in the following paragraphs.

The governing bending equation in absence of shear distortion for a simply supported member loaded at its center is given in (12). Similarly, (13) is the governing stress equation. Re-arranging these two equations and setting them equal to one another results in (14).

$$\Delta = \frac{P(L^3)}{48(EI)} \tag{12}$$

$$\sigma = \varepsilon(E) = \frac{M(c)}{I} \tag{13}$$

$$\frac{\varepsilon}{\Delta} = \frac{12(c)}{L^2} \tag{14}$$

Δ is vertical deflection; P is the applied load; L is the clear span; E is the elastic modulus; I is the moment of inertia; σ is the tensile stress; M is the bending moment; and c is the distance from the neutral axis to outermost fiber of the specimen.

Substituting the geometric properties of the components being studied results in an (/Δ) of 1.31E-4. This constant can be viewed as a geometric property that would be achieved in absence of deflection due to shear. However, FRP materials are prone to shear deflection. When viewed in the manner presented, the extent a given shape, fiber architecture, and resin matrix combination is prone to shear deflection can be reliably computed using instrumented testing in the absence of highly complicated numerical analysis. As seen in Figure 3(f), (ε /Δ) values of 1.17E-4 and 0.98E-4 occur for the polyester and vinylester components, respectively. Taking the value 1.31E-4 then dividing it by the aforementioned values results in factors of 1.12 and 1.34 for the polyester and vinylester components, respectively. The deflection of the components would need to be reduced by these factors to eliminate shear deflection. Stated another way, [1-1/1.34]*100 or 25% of the deflection of the vinylester component is due to shear, and [1-1/1.12]*100 or 11% of the polyester component deflection is due to shear.

The method presented produced values that fall in line with the values reported in [6] where the lesser (L/r) components experienced proportionally more shear deflection. The polyester- component results were found to be similar to the values reported by Neto and La Rovere [15] for the same (L/r) ratio and fiber type. Therein, an apparent modulus accounting for only flexural deformation was compared to a true modulus accounting for overall behavior. The result for an (L/r) ratio of 40 was just over 0.9, which could loosely be interpreted just under 10% deformation due to shear.

VI. CONCLUSION

A practical approach to evaluating thin-walled-FRP-bridge-deck components has been presented. The methodology is a combination of instrumented testing and fundamental principles, but does not make use of highly sophisticated numerical simulations requiring large numbers of inputs and computational power. The approach was successful in assessing behavior of bridge deck components in terms of

bending and torsion.

Approximate Classical Lamination Theory was used to compute the shear moduli of the components, which was then used in conjunction with instrumented testing to determine the Saint-Venant torsion constant *J*. The value computed was 3.16E-04 m^4, which is a reasonable value for the shape under consideration. To compute the value theoretically would be a rigorous exercise. Testing showed the FRP-component-bending stiffness was not reduced by simultaneous torsion and bending within the elastic range.

Fundamental stress and deflection relationships were used in conjunction with instrumented testing to determine the influence of shear deformation. Shear deformation accounted for 25% of the total vinylester component deflection and 11% of the total polyester component deflection. These values are reasonable and align with other values reported for thin-walled FRP materials.

VII. ACKNOWLEDGMENT

The author thanks the Constructed Facilities Center at West Virginia University for support of this project. The author especially thanks Dr. Hota V. GangaRao for his contributions to the project and also for his contributions to the author.

VIII. REFERENCES

[1] FHWA (2006). *Status of the Nation's Highways, Bridges, and Transit: Conditions and Performance.* <http://www.fhwa.dot.gov/policy/2006cpr/chap3.htm#bridge> *(Dec 20, 2007).*

[2] A. K. Maji, L. Sanchez, and R. Acree, "Processing variables and their effects on pultruded composites," *Journal of Advanced Materials,* 131(4), pp. 14-26, 1999.

[3] H. V. S GangaRao, H. K., Thippeswamy, V., Shekar, and C. Craigo, "Development of glass fiber reinforced polymer composite bridge deck," *SAMPE Journal,* 35(4), pp. 12-24, 1999.

[4] R. E. Chambers, "Fiber-Reinforced-Plastic (FRP) Structures," *Journal of Composites for Construction,* 1(1), pp. 26-38, 1997.

[5] V. Nagaraj, *Static and fatigue response of pultruded FRP beams without and with splice connections.* MS Thesis, West Virginia University, Morgantown, WV, 1994.

[6] V. Nagaraj and H. V. S. GangaRao, "Static behavior of pultruded GFRP beams," *Journal of Composites for Construction,* 1(3), pp. 120-129, 1997.

[7] R. Lopez-Anido, *Analysis and design of orthotropic plates stiffened bylaminated beams for bridge superstructures.* PhD Dissertation, West Virginia University, Morgantown, WV, 1995.

[8] R. M. Jones, (1975). *Mechanics of Composite Materials.* Hemisphere Publishing Corp, Bristol, PA.

[9] S. Sotiropoulos, *Performance of FRP Components and Connections for Bridge Deck Systems.* PhD Dissertation, West Virginia University, Morgantown, WV, 1995.

[10] S. P. Timoshenko, and J. M. Gere, (1961). *Torsional Buckling-Theory of Elastic Stability.* McGraw-Hill, New York.

[11] T. M. Roberts and Al-Ubaidi, "Flexural and torsional properties of pultruded fiber reinforced plastic I-profiles," *Journal of Composites for Construction,* 6(1), pp. 28-34, 2002.

[12] B. Omidvar, "Shear coefficient in orthotropic thin-walled composite beams," *Journal of Composites for Construction,* 2(1), pp. 46-56, 1998.

[13] M. R. Usal, M. Usal, and U. Esendemir, "Static and dynamic analysis of simply supported beams," *Journal of Reinforced Plastics and Composites,* 27(3), pp. 263-276, 2008.

[14] L. C. Bank, "Properties of pultruded Fiber Reinforced Plastic structural members," *Transportation Research Record: Journal of the Transportation Research Board,* 1223, pp. 117-124, 1989.

[15] A. B .S. Neto and H. L. La Rovere, "Flexural stiffness characterization of Fiber Reinforced Plastic (FRP) pultruded beams," *Composite Structures,* vol. 81, pp. 274-282, 2007.

ABOUT THE AUTHOR

ISAAC L. HOWARD, PHD is an Assistant Professor in the Department of Civil and Environmental Engineering at Mississippi State University, 235 Walker Hall; PO Box 9546, Mississippi State, MS, 39762. (662) 325-7193 (ph); (662) 325-7189 (fax)